Saturation physics in ultra high energy cosmic rays: heavy quark production

Victor P. Gonçalves

Instituto de Física e Matemática, Universidade Federal de Pelotas
Caixa Postal 354, CEP 96010-900, Pelotas, RS, Brazil
E-mail: `barros@ufpel.edu.br`

Magno V.T. Machado

Centro de Ciências Exatas e Tecnológicas, Universidade Federal do Pampa
Campus de Bagé, Rua Carlos Barbosa. CEP 96400-970. Bagé, RS, Brazil
E-mail: `mmachado.unipampa@ufpel.edu.br`

Abstract: In this work we estimate the heavy quark production in the interaction of ultra high energy cosmic rays in the atmosphere, considering that the primary cosmic ray is a proton or a photon. At these energies the saturation momentum $Q^2_{\mathrm{sat}}(x)$ stays above the hard scale $\mu_c^2 = 4m_c^2$, implying charm production probing the saturation regime. In particular, we show that the ep HERA data presents a scaling on $\tau_c \equiv (Q^2 + \mu_c^2)/Q^2_{\mathrm{sat}}(x)$. We derive our results considering the dipole picture and the Color Glass Condensate formalism, which one shows to be able to describe the heavy quark production in γp and pp collisions. Nuclear effects are considered for the scattering of primaries with the air nuclei and we provide a parametrization for the charm and bottom differential cross sections, $d\sigma/dx_F$, which can be used as an input for numerical implementations for lepton flux. Implications on the flux of prompt leptons at the Earth are analyzed and a large suppression is predicted.

Contents

1. Introduction

Ultra high energy cosmic rays (UHECRs) remain a puzzle in physics. Although the existence of UHECRs with energies above 10^{20} eV is now a well-established fact, the theoretical understanding of its origin and propagation is a subject of strong interest and intense discussion [1]. In general terms the current theories for the origin of UHECRs can be classified in two distinct scenarios. In the Bottom-Up scenario, charged particles are accelerated from lower energies to high energies in astrophysical environments. On the other hand, in the Top-Down scenario, the energetic particles arise from decay of massive particles originating from physical processes in the early Universe. Another open question is the basic composition of the UHECRs. While in the Bottom-Up models the primaries are accelerated protons (or nuclei), the Top-Down models predict an increasing photon component at energies above $10^{19.7}$ eV. Indeed, even in bottom-up models ultra high energy photons are expected from the GZK process during the cosmic ray propagation [2]. Finally, the interaction of the UHECRs with the atmosphere nuclei probes the theory of the strong interactions in a new kinematical range characterized by a center of mass energy of approximately 500 TeV, which is more than one order of magnitude larger than the future Large Hadron Collider at CERN.

An important subject in cosmic ray physics is the flux of prompt leptons at the Earth which reflects the primary interactions at energies that can by far exceed the highest available energies. Its quantification is essential for the cosmic ray physics as well as for neutrinos physics. On one hand, the flux of cosmic ray muons in the atmosphere, underground and underwater provides a way to testing the inputs of nuclear cascade models, that is, parameters of the primary cosmic ray flux (energy spectrum, chemical composition, ...) and particle interactions at high energies [3]. On the other hand, the flux of atmospheric neutrinos and muons at very high energies provides the main background of searches for the muons neutrinos from extra-galactic neutrino sources in the neutrinos

experiments (e.g. AMANDA, Antares, Nestor), limiting the sensitivity of any neutrino telescope to astrophysical signals [4].

The flux of prompt leptons is directly associated to the charmed particle production and its decays, whose estimation is strongly dependent on the model used to calculate the charm production cross section and energy spectra [5 – 8]. It is related to the need of extrapolating charm production data obtained at accelerators energies to the order of magnitudes higher energies of the relevant cosmic rays collisions. Another uncertainty present in the estimate of prompt lepton fluxes is associated to the fact that different authors do not use the same atmospheric particle showering routines, turning the comparison among their predictions even more difficult (See e.g. ref. [9]).

Over the past few years, the heavy quark production at colliders has received considerable attention. In particular, the compatibility among perturbative QCD (pQCD) and experimental data was verified and today one can conclude that even for charm, whose low mass and larger non-perturbative hadronisation corrections might cast doubts on the predictive power of the theory, pQCD actually manages to deliver good results. This framework was used in the prompt lepton fluxes calculations presented in refs. [5 – 8]. However, since the lepton fluxes are strongly dependent on the behavior of the gluon distribution at small-x [10] and it is determined by the QCD dynamics, we have that any new dynamical effect will modify the estimates of the lepton fluxes. Recent results at the DESY electron-proton collider HERA indicate the presence of the parton saturation effects (See e.g. ref. [12]), which modify the linear DGLAP dynamics [11]. Furthermore, a current open question is related to the possibility of the breakdown of the collinear factorization at higher energies due to saturation effects which are expected to be present in this regime [13, 14]. As in the previous calculations [5 – 8] the authors have assumed the validity of the collinear factorization and gluon distributions which are solution from the DGLAP evolution equation, we believe that a new study of the prompt lepton flux is timely and necessary.

In this paper we estimate the heavy quark production considering the present understanding of the high energy regime of the theory of strong interactions (For recent reviews see ref. [12]). In this regime, perturbative Quantum Chromodynamics (pQCD) predicts that the small-x gluons in a hadron wavefunction should form a Color Glass Condensate (CGC), which is characterized by the limitation on the maximum phase-space parton density that can be reached in the hadron wavefunction (parton saturation), with the transition being specified by a typical scale, which is energy dependent and is called saturation scale Q_{sat}. In order to estimate the saturation effects we calculate the heavy quark production using the color dipole approach, which gives a simple unified picture for this process in photon-hadron and hadron-hadron interactions. Beside charm production we also estimate the bottom production, since B-hadrons can also contribute to the τ and ν_τ fluxes. It is important to emphasize that differently of the charm quark production in the current accelerators, where the saturation scale Q_{sat} is smaller than the typical hard scale, $\mu_Q = 2m_Q$, at the energies of interest in this paper, $E > 10^{18}$ eV, we will probe for the first time the kinematical regime where $Q_{sat} > \mu_c$. Therefore, at these energies one can expect a large modification of the charm quark total cross sections and, consequently, on the flux of prompt leptons at the Earth.

Here we restrict ourselves to estimate the heavy quark production considering the present understanding of the high energy regime of the theory of strong interactions and to predict the magnitude of the saturation effects in the main quantities which are used as input in the atmospheric particle shower routines. As the theoretical predictions of the prompt leptons depend strongly on the behavior of the total cross section for heavy quark production at high energies, we believe that this partial calculation allow us to obtain a reasonable estimate of the magnitude of the saturation effects on prompt lepton flux at the Earth. Of course, more detailed studies are necessary in future in order to get precise predictions. This paper is organized as follows. In the next section we present a brief review of the heavy quark production in the color dipole picture, demonstrating the direct relation between the total heavy quark cross sections and the dipole-target cross section σ_{dip}. The QCD dynamics is discussed in section 3 and the phenomenological model for σ_{dip} used in our calculations is presented. In the section 4 we present our results and our main conclusions are summarized in the section 5.

2. Heavy quark production in the dipole picture

Let us start the analyzes considering the heavy quark production in photon-hadron interactions at high energies. It is usually described in the infinite momentum frame of the hadron in terms of the scattering of the photon off a sea quark, which is typically emitted by the small-x gluons in the proton. However, in order to disentangle the small-x dynamics of the hadron wavefunction, it is more adequate to consider the photon-hadron scattering in the dipole frame, in which most of the energy is carried by the hadron, while the photon has just enough energy to dissociate into a quark-antiquark pair before the scattering. In this representation the probing projectile fluctuates into a quark-antiquark pair (a dipole) with transverse separation $\boldsymbol{r}$ long after the interaction, which then scatters off the proton [15]. In this approach the heavy quark photoproduction cross section reads as,

$$\sigma\left(\gamma p \to Q\overline{Q}X\right) = \int dz\, d^2\boldsymbol{r}\, |\Psi_T^\gamma(z,\, \boldsymbol{r},\, Q^2=0)|^2\, \sigma_{\mathrm{dip}}(x, \boldsymbol{r}), \qquad (2.1)$$

where $\Psi_T^\gamma(z,\, \boldsymbol{r},\, Q^2)$ is the transverse light-cone wavefunction of the photon which is given by [15]

$$|\Psi_T^\gamma(z,\, \boldsymbol{r},\, Q^2=0)|^2 = \frac{6\alpha_{\mathrm{em}}}{4\,\pi^2}\, e_Q^2\, \left\{ [z^2 + (1-z)^2]\, \varepsilon^2\, K_1^2(\varepsilon\, r) + m_Q^2\, K_0^2(\varepsilon\, r) \right\} \qquad (2.2)$$

where the quantity $\varepsilon^2 = z(1-z)\, Q^2 + m_Q^2$ depends on the heavy quark mass, m_Q. The $K_{0,1}$ are the McDonald function. The variable $\boldsymbol{r}$ defines the relative transverse separation of the pair (dipole), whereas z and $\bar{z} \equiv (1-z)$ is the longitudinal momentum fractions of the quark and antiquark, respectively. The dipole cross section, σ_{dip}, parameterizes the cross section for the dipole-target (nucleon or nucleus) interaction. As usual, the Bjorken variable is denoted by x.

Concerning heavy quark hadroproduction, it has been usually described considering the collinear factorization, with the behavior of the total cross section at high energies being

determined by the gluon-gluon fusion mechanism and the gluon distribution at small-x. However, at large energies this process can be described in terms of the color dipole cross section, similarly to photon-hadron interactions, using the color dipole formalism [16]. In this approach the total heavy quark production cross section is given by [16]

$$\sigma(pp \to Q\bar{Q}X) = 2 \int_0^{-\ln(\frac{2m_Q}{\sqrt{s}})} dy \, x_1 G\left(x_1, \mu_F^2\right) \times \sigma(GN \to Q\bar{Q}X) \,, \qquad (2.3)$$

where $y = \frac{1}{2}\ln(x_1/x_2)$ is the rapidity of the pair, $\mu_F \sim m_Q$ is the factorization scale, $x_1 G(x_1, \mu_F^2)$ is the projectile gluon density at scale μ_F and the partonic cross section $\sigma(GN \to Q\bar{Q}X)$ is given by

$$\sigma(GN \to Q\bar{Q}X) = \int dz \, d^2\boldsymbol{r} \left|\Psi_{G \to Q\bar{Q}}(z, \boldsymbol{r})\right|^2 \sigma_{q\bar{q}G}(z, \boldsymbol{r}), \qquad (2.4)$$

with $\Psi_{G \to Q\bar{Q}}$ being the pQCD calculated distribution amplitude , which describes the dependence of the $|Q\bar{Q}\rangle$ Fock component on transverse separation and fractional momentum. It is given by

$$\left|\Psi_{G \to Q\bar{Q}}(z, \boldsymbol{r})\right|^2 = \frac{\alpha_s(\mu_R)}{(2\pi)^2} \left\{ m_Q^2 \mathrm{K}_0^2(m_Q r) + \left[z^2 + \bar{z}^2\right] m_Q^2 \mathrm{K}_1^2(m_Q r) \right\},$$

where $\alpha_s(\mu_R)$ is the strong coupling constant, which is probed at a renormalization scale $\mu_R \sim m_Q$. Moreover, $\sigma_{q\bar{q}G}$ is the cross section for scattering a color neutral quark-antiquark-gluon system on the target and is directly related with the dipole cross section as follows

$$\sigma_{q\bar{q}G} = \frac{9}{8} \left[\sigma_{\mathrm{dip}}(x_2, z\boldsymbol{r}) + \sigma_{\mathrm{dip}}(x_2, \bar{z}\boldsymbol{r})\right] - \frac{1}{8}\sigma_{\mathrm{dip}}(x_2, \boldsymbol{r}). \qquad (2.5)$$

The basic idea on this approach is that at high energies a gluon G from the projectile hadron can develop a fluctuation which contains a heavy quark pair $(Q\bar{Q})$. Interaction with the color field of the target then may release these heavy quarks. In ref. [17] the equivalence between this approach and the gluon-gluon fusion mechanism of the conventional collinear factorization has been demonstrated. In particular, the dipole predictions are similar to those obtained using the next-to-leading order parton model calculation. Moreover, the predictions for heavy quark production agree well with the current experimental data.

It is important to emphasize that the color dipole picture is valid for high energies, where the coherence length $l_c \approx 1/x_2$ is larger than the target radius. At smaller energies, we should include, for instance, the quark-antiquark contributions. However, at high energies the dipoles with fixed transverse separations are the eigenstates of interaction in QCD, which becomes the eikonalization an exact procedure, allowing a direct generalization of the approach to calculate the heavy quark production in photon-nucleus and proton-nucleus collisions. Moreover, this approach is the natural framework to include the saturation effects. Another aspects that should be emphasized are that (i) in this formalism a K-factor is not necessary, since is includes all higher-twist and next-to-leading corrections; (ii) the dipole cross section is universal, i.e., it is process independent.

3. High energy QCD dynamics

The Color Glass Condensate is described by an infinite hierarchy of coupled evolution equations for the correlators of Wilson lines [18]. In the absence of correlations, the first equation in the Balitsky-JIMWLK hierarchy decouples and is then equivalent to the equation derived independently by Kovchegov within the dipole formalism [19]. In the CGC formalism σ_{dip} can be computed in the eikonal approximation, resulting

$$\sigma_{\mathrm{dip}}(x, \boldsymbol{r}) = 2 \int d^2 \boldsymbol{b} \, \mathcal{N}(x, \boldsymbol{r}, \boldsymbol{b}) \, , \qquad (3.1)$$

where $\mathcal{N}$ is the dipole-target forward scattering amplitude for a given impact parameter $\boldsymbol{b}$ which encodes all the information about the hadronic scattering, and thus about the non-linear and quantum effects in the hadron wave function. It is useful to assume that the impact parameter dependence of $\mathcal{N}$ can be factorized as $\mathcal{N}(x, \boldsymbol{r}, \boldsymbol{b}) = \mathcal{N}(x, \boldsymbol{r}) S(\boldsymbol{b})$, so that $\sigma_{\mathrm{dip}}(x, \boldsymbol{r}) = \sigma_0 \mathcal{N}(x, \boldsymbol{r})$, with σ_0 being a free parameter related to the non-perturbative QCD physics. The Balitsky-JIMWLK equation describes the energy evolution of the dipole-target scattering amplitude $\mathcal{N}(x, \boldsymbol{r})$. Although a complete analytical solution is still lacking, its main properties are known: (a) for the interaction of a small dipole ($\boldsymbol{r} \ll 1/Q_{\mathrm{sat}}$), $\mathcal{N}(\boldsymbol{r}) \approx \boldsymbol{r}^2$, implying that this system is weakly interacting; (b) for a large dipole ($\boldsymbol{r} \gg 1/Q_{\mathrm{sat}}$), the system is strongly absorbed and therefore $\mathcal{N}(\boldsymbol{r}) \approx 1$. The typical momentum scale, $Q_{\mathrm{sat}}^2 \propto x^{-\lambda}$ ($\lambda \approx 0.3$), is the so called saturation scale. This property is associated to the large density of saturated gluons in the hadron wave function. In our analysis we will consider the phenomenological saturation model proposed in ref. [20] (including fit with charm quark) which encodes the main properties of the saturation approaches, with the dipole cross section parameterized as follows

$$\sigma_{\mathrm{dip}}^{\mathrm{CGC}}(x, \boldsymbol{r}) = \sigma_0 \begin{cases} \mathcal{N}_0 \left(\frac{\bar{\tau}^2}{4} \right)^{\gamma_{\mathrm{eff}}(x, r)} \, , & \text{for } \bar{\tau} \leq 2 \, , \\ 1 - \exp \left[-a \, \ln^2 (b \, \bar{\tau}) \right] \, , & \text{for } \bar{\tau} > 2 \, , \end{cases}$$

where $\bar{\tau} = \boldsymbol{r} Q_{\mathrm{sat}}(x)$ and the expression for $\bar{\tau} > 2$ (saturation region) has the correct functional form, as obtained from the CGC formalism [18]. For the color transparency region near saturation border ($\bar{\tau} \leq 2$), the behavior is driven by the effective anomalous dimension $\gamma_{\mathrm{eff}}(x, r) = \gamma_{\mathrm{sat}} + \frac{\ln(2/\bar{\tau})}{\kappa \lambda \ln(1/x)}$, where $\gamma_{\mathrm{sat}} = 0.63$ is the LO BFKL anomalous dimension at saturation limit and $\kappa = 9.9$. Hereafter, we label this model by CGC.

In the case of photon-nucleus and hadron-nucleus interactions we take the Glauber-Gribov formalism for nuclear shadowing, with an average mass number $A = 14.5$. This is done by replacing σ_{dip} for a nucleon by a nuclear dipole cross section,

$$\sigma_{\mathrm{dip}}^{\mathrm{nucl}} = 2 \int d^2 b \, \left[1 - \exp \left(-\frac{1}{2} A T_A(b) \, \sigma_{\mathrm{dip}} \right) \right] \, , \qquad (3.2)$$

where $T_A(b)$ is the nuclear profile function. This approach leads a reasonable description of the current experimental data for the nuclear structure function [21].

As a shot comment, the present work is based extensively on the Color Glass Condensate. However, there is complementary approaches in literature. For instance, in ref. [22]
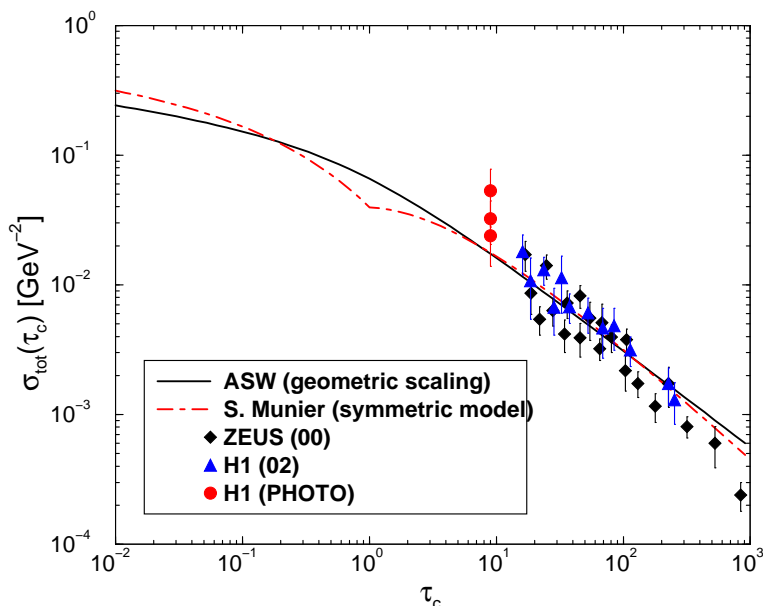
Figure 1: Experimental data on inclusive charm production at DESY-HERA plotted versus the scaling variable τ_c.

a loop-loop correlation model is able to compute hadronic cross sections in good agreement with cosmic ray data from Fly's eye and Akeno. Moreover, saturation in the impact parameter space can be explicitly investigated in that model.

4. Results for cosmic rays

Before presenting our results for the heavy quark production at very high energies let us consider a basic property of the saturation physics: the geometric scaling. When applied for the deep inelastic scattering it means that the total $\gamma^* p$ cross section at large energies is not a function of the two independent variables x and Q, but is rather a function of the single variable $\tau = Q^2/Q_{\text{sat}}^2(x)$ as demonstrated in ref. [23]. In ref. [24] we demonstrate that this property is also present in the charm experimental data at $Q^2 > 0$. In order to include the experimental data for the photoproduction of charm we have reanalyzed our results and verified that the DESY-HERA experimental data [25] at $Q^2 \geq 0$ presents the geometry scaling behavior on the variable $\tau_c \equiv (Q^2 + 4m_c^2)/Q_{\text{sat}}^2$. It is demonstrated in the figure 1, where we also present the predictions of two scaling models [27, 28], which we generalize for charm production. In the symmetric saturation model [27], scaling on τ_c has been computed before in ref. [24] and here it is generalized for the case where saturation scale is larger than μ_c. It reads as,

$$\sigma_{\text{tot}}^{c\bar{c}}(\tau_c) = \bar{\sigma} \begin{cases} 1 - \exp\left[-\frac{k}{\tau_c}\left(1 + \log\left(\tau_c\right)\right], & \text{for } \tau_c > 1, \\ \frac{1}{\tau_c} - \frac{1}{\tau_c}\exp\left[-k\tau_c\left(1 - \log\left(\tau_c\right)\right)\right], & \text{for } \tau_c \leq 1, \end{cases}$$

The parameters are taken from [27], with $k = 0.8$, and the overall normalization gives $\bar{\sigma} = 28\,\mu b$. Furthermore, we consider the model proposed in ref. [28] (hereafter ASW model),
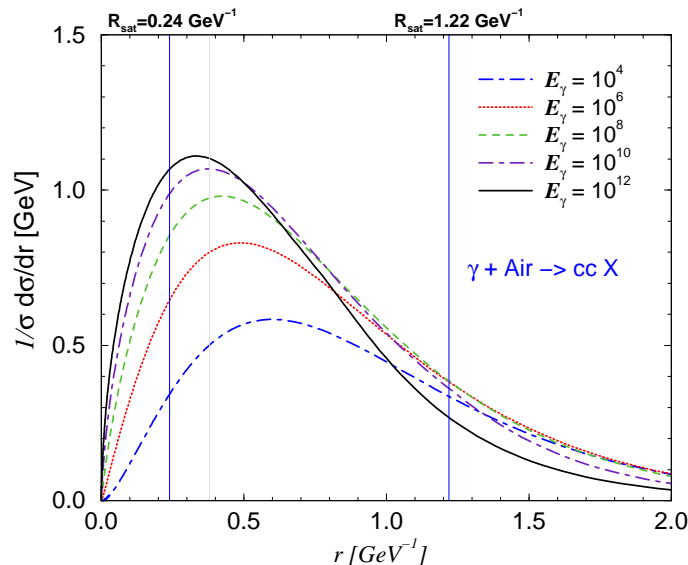
Figure 2: Profile function for charm production.

which relate the $\gamma p(A)$, pA and AA collisions through the geometric scaling property of the saturation physics. The parameters for this model has been obtained from a fit to the small-x ep DESY-HERA data and lepton-hadron data [28]. When generalized for charm production we obtain

$$\sigma_{c\bar{c}}^{\gamma^* A} = \frac{\pi R_A^2}{\pi R_p^2} \bar{\sigma}_0 \left[\gamma_E + \Gamma\left(0, \frac{a}{\tau_{A,c}^b}\right) + \ln\left(\frac{a}{\tau_{A,c}^b}\right) \right], \tag{4.1}$$

where γ_E is the Euler constant, $\Gamma(0, \beta)$ the incomplete Gamma function and R_A is the nuclear radius. The nuclear scaling variable for charm production is $\tau_{A,c} = \tau_c \left(\frac{R_A^2}{A R_p^2}\right)^\Delta$. The parameters are $a = 1.868$, $b = 0.746$, $\Delta = 1.266$, $\pi R_p^2 = 1.55\,\text{fm}^2$ and $\bar{\sigma}_0 = 20.28$ μb. Our predictions for charm production in γp processes are presented in figure 1. The agreement with experimental data is very good, which allow us to propose the eq. (4.1) as a theoretical parameterization for the charm production in lepton-nuclei interactions at very high energies.

We are ready now to investigate the charm production initiated by primary cosmic rays photons or protons interacting with atmosphere. Initially, lets consider the photon-hadron interaction and analyze the behavior of the profile function, defined by

$$\frac{1}{\sigma_{\text{tot}}} \frac{d\sigma_{Q\bar{Q}}}{dr} = \frac{4\pi r}{\sigma_{\text{tot}}} \int d^2b\,dz\, |\Psi_T^\gamma(z, \boldsymbol{r}, Q^2 = 0)|^2 \left[1 - \exp\left(-\frac{1}{2} A T_A(b)\, \sigma_{\text{dip}}(x, \boldsymbol{r}^2)\right) \right] (4.2)$$

which allow us to estimate the mean dipole size dominating the nuclear heavy quark photoproduction. In figures 2 and 3 are shown, respectively, the overlap function for the charm and bottom production as a function of dipole size. They are computed for the average mass number $A = 14.5$ and for different photon energies. In the charm case, the distributions are peaked at approximately $r \approx 0.4\,\text{GeV}^{-1}$, whereas for the bottom case this
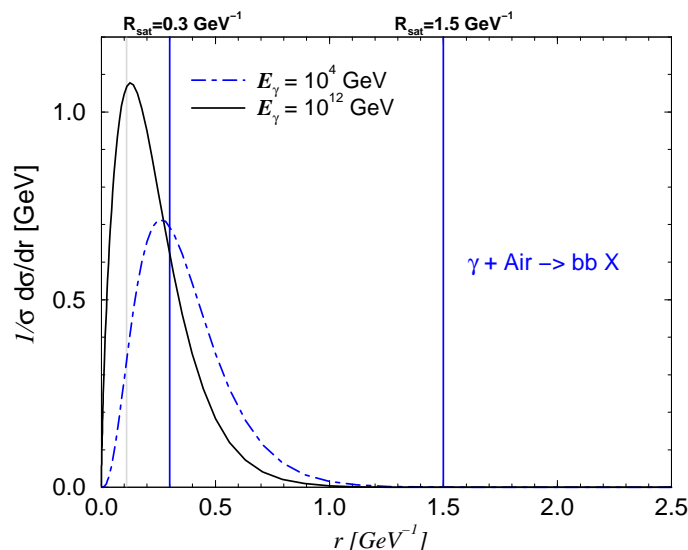
Figure 3: Profile function for bottom production.

value is shifted to $r \approx 0.1 \, \mathrm{GeV}^{-1}$, which agree with the theoretical expectation that the $q\bar{q}$ pairs have a typical transverse size $\approx 1/2m_f$ [15]. Therefore, the main contribution to the cross section comes from the small dipole sizes, i.e. from the perturbative regime. In contrast, for light quarks a broader r distribution is obtained, peaked for large values of the pair separation, implying that nonperturbative contributions cannot be disregarded in that case. We also show in the figures the corresponding nuclear saturation radius, estimated in a simple way as $R_{\mathrm{sat}} \simeq A^{-1/6}/Q_{\mathrm{sat}}(\bar{x})$, where $\bar{x} = \frac{4\,m_Q^2}{W_{\gamma A}^2}$ and $W_{\gamma A}^2 = 2m_N E_\gamma$, for two different values of the photon energy E_γ. For the charm case we have that at low energies ($E_\gamma = 10^4 \, \mathrm{GeV}$) the distribution is peaked at values smaller than the corresponding R_{sat}, which implies that the saturation effects can be disregarded in this regime. On the other hand, for high photon energies ($E_\gamma = 10^{12} \, \mathrm{GeV}$) we have that the peak occurs at larger values than R_{sat} and the saturation effects are expected to contribute for the total cross section. In contrast, for the bottom case, we have that for all energy range considered the peaks occur at smaller values than R_{sat}, which implies that these effects do not contribute too much for the bottom contribution.

In figures 4 and 5 we show the charm and bottom photoproduction cross sections as a function of photon energy, respectively. The γp interaction is obtained via eq. (2.1) with the dipole-proton cross section given by $\sigma_{\mathrm{dip}}^{\mathrm{CGC}}$. The experimental data from HERA [25] and fixed target collisions [26] are also included for sake of comparison. The theoretical curves roughly describe the data, which have large uncertainties and large errors. We call attention that the CGC model successfully describes the charm and bottom electroproduction data (even at small Q^2) and so we believe in its robustness. Therefore, accurate new experimental measurements in this region is of particular importance.

As explained in the previous section, for the photon-air interaction we take the Glauber-Gribov formalism for nuclear shadowing, with an average mass number $A = 14.5$ and σ_{dip}
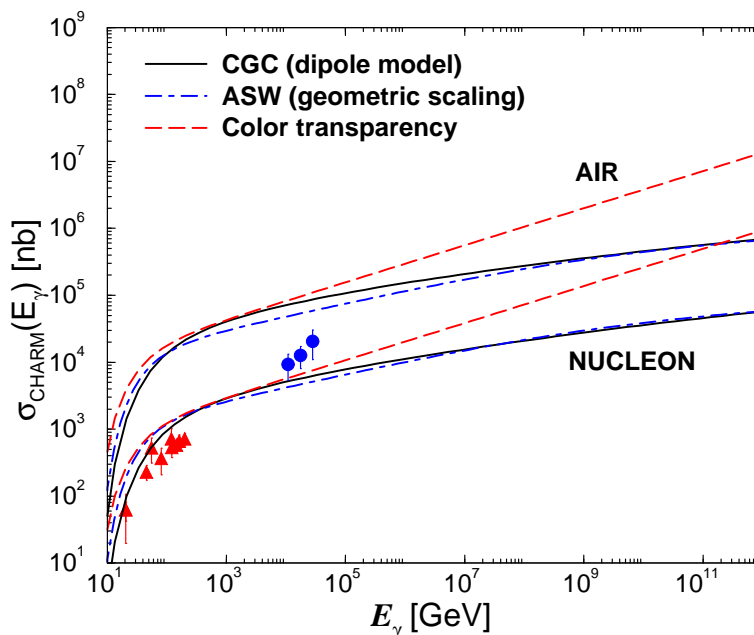
Figure 4: Charm production in γp and γA interactions. Data from refs. [25, 26].

replaced by $\sigma_{\rm dip}^{\rm nucl}$. Initially, lets discuss the nuclear charm photoproduction. In figure 4 the accelerator data [25] and the predictions of our theoretical parameterization, eq. (4.1), are also presented. The energy dependence is mild at $E_\gamma \geq 10^5\,{\rm GeV}$, giving $\sigma \propto E_\gamma^{0.12}$. The parameterization is numerically equivalent to the complete CGC dipole calculation, which can be useful as input in Monte Carlo implementations. In order to estimate the magnitude of the saturation corrections to the high energy process, we also show the result using the color transparency (long dashed curves) calculation, which corresponds to the leading twist contribution $\sigma_{\rm dip} \propto r^2\, xG(x, 1/r^2)$. The deviation are about one order of magnitude at $E_\gamma \approx 10^{12}\,{\rm GeV}$, increasing for higher energies. Therefore, in agreement with the previous analyzes of the profile function, parton saturation plays an important role in charm production by cosmic rays interactions when the primary particle is a photon.

Concerning to nuclear bottom photoproduction, our results are presented in figure 5. We have that the contribution of the saturation effects is smaller, being of approximately 10 % at very high photon energies ($E_\gamma \approx 10^{12}\,{\rm GeV}$). This result agree with our previous analyzes of the profile function. An important aspect is that the growth with the energy of the bottom cross section is steeper than the charm case due to distinct physics which is dominant in the production process (linear versus saturation physics). It implies that the contribution for the prompt lepton fluxes associated to the bottom becomes more important for larger energies.

Lets now consider that the primary cosmic ray is a proton and estimate the heavy quark production cross section in this case. In Fig 6 we show the theoretical predictions for charm quark production in proton-proton and proton-air interactions as a function of energy of primary cosmic rays. The solid curves correspond to the calculation using eq. (2.3), with
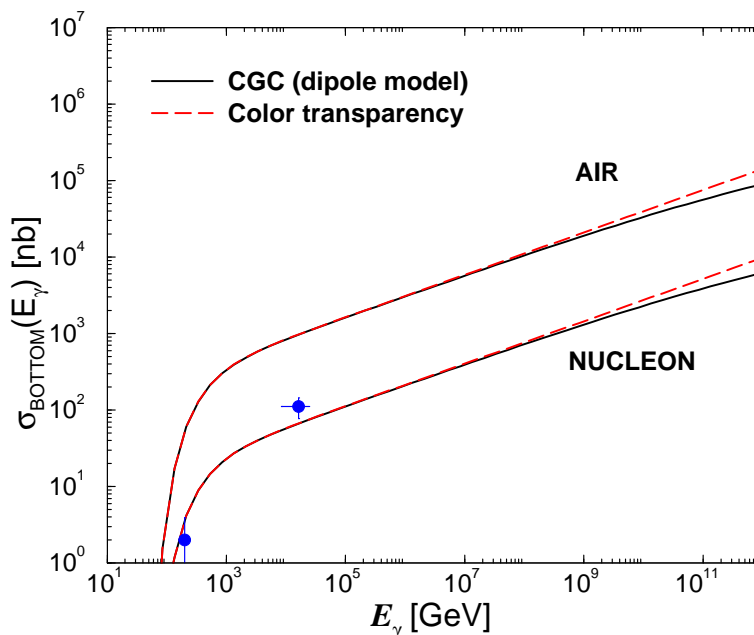
Figure 5: Bottom production in γp and γA interactions. Data from refs. [25, 26].

gluon distribution given by the NLO "physical gluon" MRST2004 parameterization [29]. The accelerator data [30] and the color transparency (long dashed curves) calculation are also presented. We have that the current data at high energies are well described using the color dipole picture and that for the energy range of the data the color transparency and CGC prediction are almost identical. The energy dependence is suddenly steeper than the photon case, with $\sigma \propto E_p^{0.17}$ at $E_p \geq 10^7$ GeV. The deviation between CGC and leading twist approaches remains large, being of order of six at $E_p \approx 10^{12}$ GeV and increasing with energy. It confirms the importance of parton saturation corrections in charm quark production via cosmic rays.

In ref. [10] the authors have computed the total cross section for charm production using the collinear factorization, next-to-leading order corrections and different parton distribution parameterizations. In particular, the dependence of the predictions in the behavior of the gluon distribution at small-x was analyzed in detail. In comparison with those results we have that our predictions considering the color transparency limit are similar with the MRST one for $\lambda = 0.2$ (See figure 1 in ref. [10]). On the other hand, our predictions considering the saturation effects are very similar to those obtained previously by Thunman, Ingelman and Gondolo (TIG) [5], which have used an option of PYTHIA by which the gluon distribution is extrapolated for $x \leq 10^{-4}$ with $\lambda = 0.08$. As discussed before, the prompt lepton fluxes are strongly dependent on the charm cross section. Consequently, we can expect that if our results are used as input in the atmospheric particle shower routines, the predicted prompt lepton flux should be similar to the TIG predictions, which have been considered a lower bound for the flux of leptons obtained using pQCD. In other words, we have that the saturation physics on charm quark production implies a
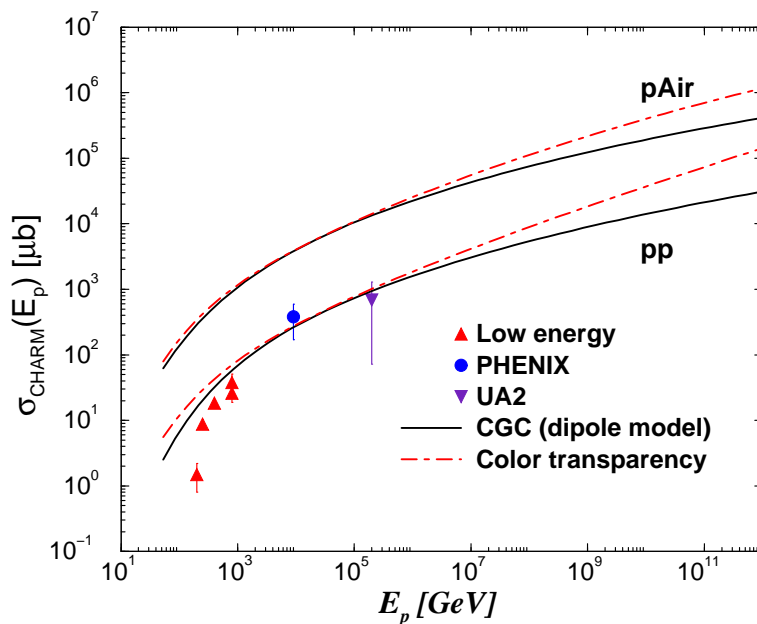
Figure 6: Charm production in pp and pA interactions. Data from ref. [30].
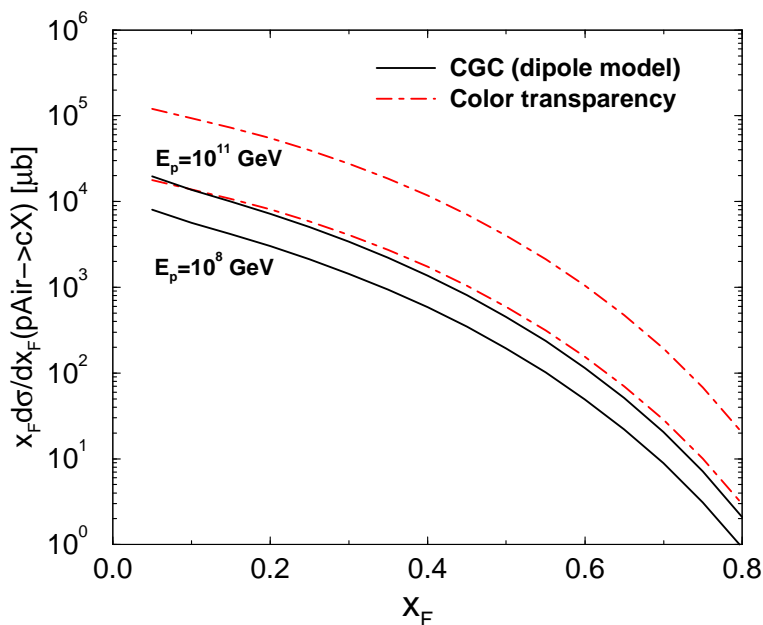

Figure 7: Comparison of the CGC and color transparency predictions for the x_F-dependence for charm production in pA interactions.

suppression of the prompt lepton fluxes.

In what follows we analyze the behavior of the x_F-distribution for charm production, $x_F d\sigma^c/dx_F$, which is necessary to calculate the charm production spectrum-weighted moment, also called production "Z-moment". The x_F-distribution can be directly obtained

Energy Range	a_0	a_1	b_0	b_1	n_0	n_1
$10^4 < E_p < 10^8$ GeV	6804 μb	826	0.05	0.016	0.075	-0.107
$10^8 < E_p < 10^{11}$ GeV	5422 μb	403	0.025	0.023	6.7	-0.102

Table 1: Parameters of the fit to the differential cross section $x_F \, d\sigma/dx_F$ for charm production in proton-air collisions (see text).

from the rapidity distribution in color dipole approach, which is given by [16]

$$\frac{d\sigma(pp \to Q\bar{Q}X)}{dy} = x_1 G\left(x_1, \mu_F^2\right) \sigma(GN \to Q\bar{Q}X). \tag{4.3}$$

Using that $x_F = x_1 - x_2$ and $y = \frac{1}{2}\ln(x_1/x_2)$ one obtain $x_F = \frac{2M_{Q\bar{Q}}}{\sqrt{s}} \sinh y$, where $M_{Q\bar{Q}}$ is the invariant mass of the heavy quarks pair and the momentum fractions are given by $x_{1,2} = (\sqrt{x_F^2 + \frac{4M_{Q\bar{Q}}}{s}} \pm x_F)/2$. Consequently, the x_F-distribution is

$$\frac{d\sigma(pp \to Q\bar{Q}X)}{dx_F} = \frac{\sqrt{s}}{\sqrt{\left(2M_{Q\bar{Q}}\right)^2 + (\sqrt{s}x_F)^2}} \frac{d\sigma(pp \to Q\bar{Q}X)}{dy}. \tag{4.4}$$

The extension to scattering on nuclei is straightforward by replacing $\sigma(GN \to Q\bar{Q}X)$ for $\sigma(GA \to Q\bar{Q}X)$. It is important to emphasize that the heavy quark production actually contains two different phases, which are not unambiguously separable: the first is the description of the heavy quark in the hard collision which we have addressed above; the second is the non-perturbative fragmentation into a heavy hadron, which cannot be calculated and are in general extracted from the e^+e^- data. In our study we do not include the hadronization of the heavy quarks, since it is model dependent. Of course, in a full calculation it should be considered.

In figure 7 we present this distribution for two values of the proton energy considering the saturation effects (CGC) and the color transparency limit. As expected, the difference between the predictions increases with the energy, being of approximately one order of magnitude for $E_p = 10^{11}$ GeV. In figure 8 we present the CGC predictions for the x_F-distribution and different values of energy. The shape of the distribution becomes a little steeper as the energy increases. In order to allow future studies of the prompt lepton fluxes considering saturation physics we have parameterized the x_F-distribution for charm production considering the following general form

$$x_F \frac{d\sigma(p + Air \to c + X)}{dx_F} = A \, x_F^{\alpha} \, (1 - x_F^{1.2})^n, \tag{4.5}$$

with the quantities

$$A = a_0 + \left[a_1 \ln\left(\frac{E_p}{10^8 \, \text{GeV}}\right)\right], \quad \alpha = b_0 - b_1 \ln\left(\frac{E_p}{10^4 \, \text{GeV}}\right), \quad n = n_0 + n_1 \ln\left(\frac{E_p}{10^4 \, \text{GeV}}\right). \tag{4.6}$$

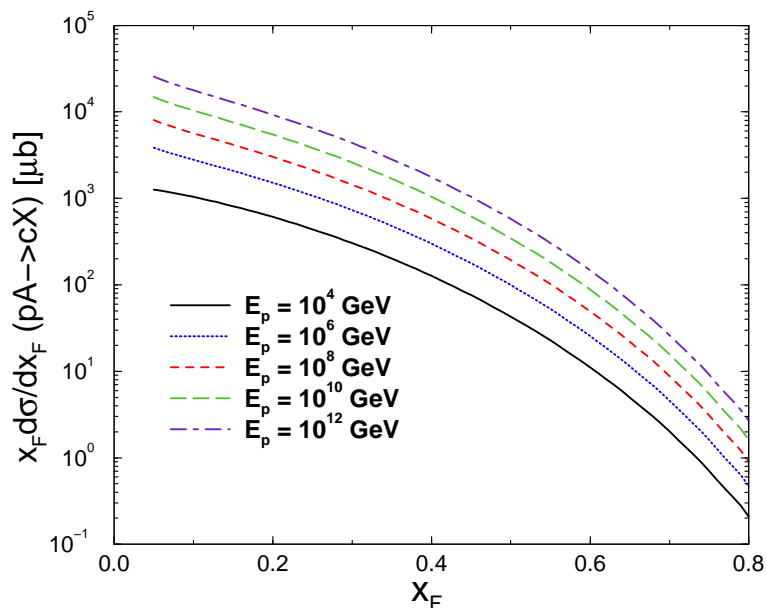The parameters for two distinct energy ranges are presented in the table 1.

Figure 8: x_F-dependence for charm production in pA interactions predicted by saturation physics.

Let us consider now the bottom production cross section and its x_F-dependence considering the color dipole picture and saturation physics. From the previous discussion we have that these effects are expected to be minimal and that the cross section is dominated by the color transparency regime. However, we present our predictions obtained using color dipole picture and an eikonalized dipole-nuclei cross section, in order to establish the results which comes from this framework. As emphasized in ref. [8], the high energy production of ν_τ from beauty decays is not negligible, what motivates our study. In figure 9 we present our predictions for the energy dependence of the total bottom production cross section considering the CGC and color transparency limit. As expected, we have that in the energy range considered in this work both predictions are almost identical for proton-proton and proton-nucleus interactions. In figure 10 the x_F-distribution is shown for different proton energies. The behavior is similar to that obtained for charm production considering the color transparency limit, with the distribution becoming steeper for larger energies. As for the charm case we have parameterized this distribution considering the general form given in eq. (4.5). The resulting parameters are presented in the table 2 for two distinct energy ranges. It important to emphasize that similarly to the photoproduction case the bottom cross section increases with the energy faster than the charm one, due to distinct physics which is dominant in the production process. In order to illustrate this feature, we have estimated the ratio of the bottom and charm cross sections for proton-air collisions as a function of proton energy for $E_p \geq 10^8 \, \text{GeV}$ and verified that it is proportional to $R_{b/c} \propto E_p^{0.1}$. Basically, we have that the bottom production cross section is increasingly important and reaches 10-13 % of the charm cross section for ultra-high energy cosmic rays. Consequently, the contribution for the prompt lepton fluxes associated to the bottom becomes important for larger energies.
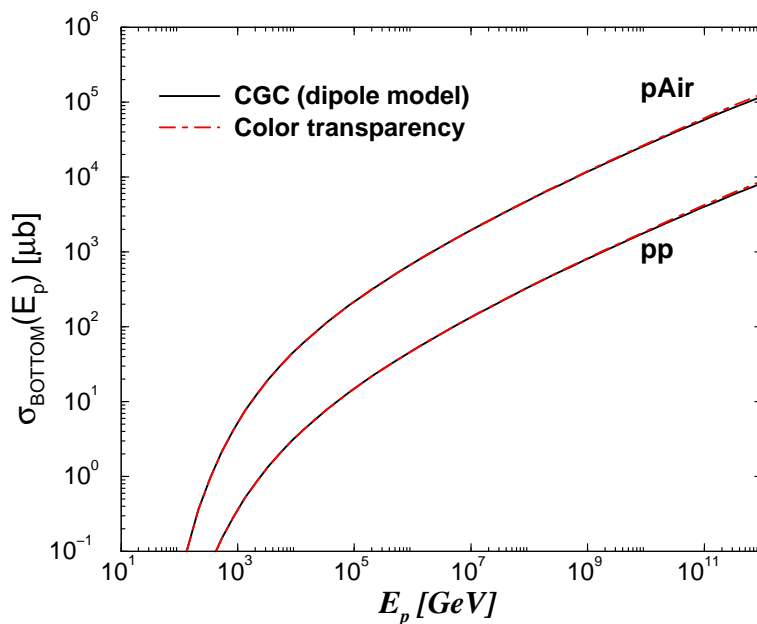
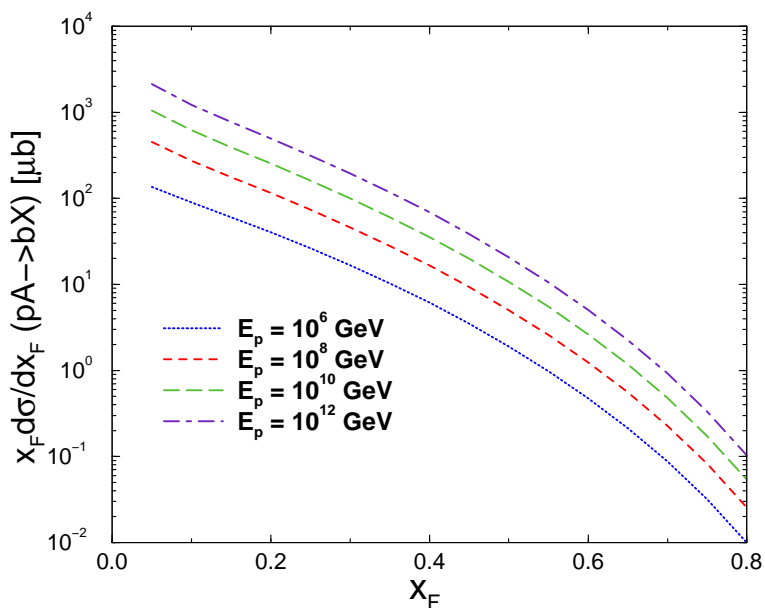**Figure 9:** Bottom production in pp and pA interactions.

Figure 10: x_F-dependence for bottom production in pA interactions.

5. Summary

The determination of the prompt lepton flux is fundamental in order to establish, for instance, the background for ultra high energy neutrinos from cosmological sources. At high energies the lepton fluxes are quite sensitive to the heavy quark cross section, which implies that the choice of an appropriate theoretical framework to estimate the cross section

Energy Range	a_0	a_1	b_0	b_1	n_0	n_1
$10^4 < E_p < 10^8$ GeV	180.23 μb	19.79	-0.048	0.035	7.54	-0.091
$10^8 < E_p < 10^{11}$ GeV	236.13 μb	36.20	-0.061	0.023	9.42	-0.18

Table 2: Parameters of the fit to the differential cross section $x_F \, d\sigma/dx_F$ for bottom production in proton-air collisions (see text).

in this energy range is fundamental. Previous calculations have considered perturbative QCD at next-to-leading order, assuming the validity of the collinear factorization and of the DGLAP dynamics in the kinematical range of very high energies. However, current accelerator data already have indicated the presence of new dynamical effects, associated to saturation physics. As the contribution of these effects increases with the energy, we can expect that it cannot be disregarded in the description of the interaction of ultra high energy cosmic rays with the atmosphere. Here we have estimated the heavy quark production in the interaction of cosmic rays in the atmosphere taking the primary cosmic ray as a proton or a photon. At ultra high energies and charm production the saturation scale stays above the semihard scale μ_c^2 and the process contains sizable contribution from the saturation regime. In particular, geometric scaling for charm production on the scaling variable τ_c is demonstrated using small-x DESY-HERA data. Within the color dipole approach and CGC formalism for dipole-target interaction, the parton saturation corrections are huge, suppressing the cross section by one order of magnitude for ultra-high energy primaries at $E_\gamma \approx 10^6$ GeV. We also predict a factor ten of suppression of the prompt lepton fluxes for a pure proton component for the primary cosmic ray, increasing if the primary component changes as appropriate for a Top-Down model. This suppression is also present in the x_F-distribution, which one the main inputs to the calculate the prompt lepton fluxes. The resulting predictions for the total cross section at very high energies are similar to those obtained previously by Thunman, Ingelman and Gondolo, which have been considered a lower bound. As there is a strict relation between the charm production and the prompt lepton fluxes, we believe that the resulting lepton fluxes obtained using our predictions for charm production as input of the atmospheric particle showers routines should be similar. In other words, we expect a suppression of the prompt lepton fluxes associated to the saturation physics when compared with those resulting from NLO calculations using the collinear factorization. Of course, a more detailed analyzes is necessary in order to quantify precisely this suppression. It is important to emphasize that these predictions should be considered a lower bound in the suppression, since in the CGC formalism the breaking of the factorization for heavy quark production is predicted for $Q_{\rm sat} \gg \mu_c$ [13], which implies a larger suppression.

We also estimate the bottom production considering the dipole picture and saturation physics. In this case, we have that the saturation effects can be disregarded and the color transparency limit determines the behavior of the total cross section in the energy range of interest in this paper. However, as the B-hadron decays should contribute significantly for the flux of high energy ν_τ neutrinos, the quantification of this cross section using the

color dipole picture, which is expressed in terms of the eigenstates of interaction in QCD, is useful.

We present a parameterization for the x_F-distribution for charm and bottom production resulting of our calculations. It can be useful for future calculations of the prompt lepton fluxes. The main conclusion of our phenomenological analyzes is that the saturation effects implies a suppression of prompt lepton fluxes. Of course, in a full calculation we should include the fragmentation of the heavy quark pairs into hadrons and their subsequent semileptonic decays, as well as, the propagation of the high energy particles through the atmosphere. We postponed these analyzes for a future publication.

Acknowledgments

References

[1] P. Bhattacharjee and G. Sigl, *Origin and propagation of extremely high energy cosmic rays*, *Phys. Rept.* **327** (2000) 109 [`astro-ph/9811011`];
L. Anchordoqui et al., *High energy physics in the atmosphere: phenomenology of cosmic ray air showers*, *Ann. Phys. (NY)* **314** (2004) 145 [`hep-ph/0407020`].

[2] G. Gelmini, O. Kalashev and D.V. Semikoz, *GZK photons as ultra high energy cosmic rays*, `astro-ph/0506128`.

[3] E.V. Bugaev et al., *Atmospheric muon flux at sea level, underground and underwater*, *Phys. Rev.* **D 58** (1998) 054001 [`hep-ph/9803488`].

[4] T.K. Gaisser, F. Halzen and T. Stanev, *Particle astrophysics with high-energy neutrinos*, *Phys. Rept.* **258** (1995) 173 [`hep-ph/9410384`] [Erratum *ibid.* **271** (1996) 355].

[5] P. Gondolo, G. Ingelman and M. Thunman, *Charm production and high energy atmospheric muon and neutrino fluxes*, *Astropart. Phys.* **5** (1996) 309.

[6] L. Pasquali, M.H. Reno and I. Sarcevic, *Lepton fluxes from atmospheric charm*, *Phys. Rev.* **D 59** (1999) 034020 [`hep-ph/9806428`].

[7] G. Gelmini, P. Gondolo and G. Varieschi, *Prompt atmospheric neutrinos and muons: NLO vs LO QCD predictions*, *Phys. Rev.* **D 61** (2000) 036005 [`hep-ph/9904457`].

[8] A.D. Martin, M.G. Ryskin and A.M. Stasto, *Prompt neutrinos from atmospheric c anti-c and b anti-b production and the gluon at very small x*, *Acta Phys. Polon.* **34** (2003) 3273.

[9] C.G.S. Costa, *The prompt lepton cookbook*, *Astropart. Phys.* **16** (2001) 193.

[10] G. Gelmini, P. Gondolo and G. Varieschi, *Prompt atmospheric neutrinos and muons: dependence on the gluon distribution function*, *Phys. Rev.* **D 61** (2000) 056011 [`hep-ph/9905377`].

[11] V.N. Gribov and L.N. Lipatov, *Deep inelastic e p scattering in perturbation theory*, *Sov. J. Nucl. Phys.* **15** (1972) 438;

Y.L. Dokshitzer, *Calculation of the structure functions for deep inelastic scattering and e^+e^- annihilation by perturbation theory in quantum chromodynamics. (in russian)*, *Sov. Phys. JETP* **46** (1977) 641;
G. Altarelli and G. Parisi, *Asymptotic freedom in parton language*, *Nucl. Phys.* **B 126** (1977) 298.

[12] E. Iancu and R. Venugopalan, *The color glass condensate and high energy scattering in QCD*, hep-ph/0303204;
V.P. Goncalves and M.V.T. Machado, *Parton saturation approach in heavy quark production at high energies*, *Mod. Phys. Lett.* **19** (2004) 2525 [hep-ph/0410012];
H. Weigert, *Evolution at small $x(bj)$: the color glass condensate*, *Prog. Part. Nucl. Phys.* **55** (2005) 461;
J. Jalilian-Marian and Y.V. Kovchegov, *Saturation physics and deuteron-gold collisions at RHIC*, *Prog. Part. Nucl. Phys.* **56** (2006) 104 [hep-ph/0505052].

[13] H. Fujii, F. Gelis and R. Venugopalan, *Quantitative study of the violation of $K(t)$-factorization in hadroproduction of quarks at collider energies*, *Phys. Rev. Lett.* **95** (2005) 162002 [hep-ph/0504047];
Quark pair production in high energy pA collisions: general features, *Nucl. Phys.* **A 780** (2006) 146 [hep-ph/0603099].

[14] N.N. Nikolaev and W. Schafer, *Breaking of $K(t)$-factorization for single jet production off nuclei*, *Phys. Rev.* **D 71** (2005) 014023 [hep-ph/0411365].

[15] N.N. Nikolaev and B.G. Zakharov, *Scaling properties of nuclear shadowing in deep inelastic scattering*, *Phys. Lett.* **B 260** (1991) 414; *Colour transparency and scaling properties of nuclear shadowing in deep inelastic scattering*, *Z. Physik* **C 49** (1991) 607.

[16] N.N. Nikolaev, G. Piller and B.G. Zakharov, *Inclusive heavy-flavor production from nuclei*, *Z. Phys. A* **354** (1996) 99 [hep-ph/9511384];
B.Z. Kopeliovich and A.V. Tarasov, *Gluon shadowing and heavy flavor production off nuclei*, *Nucl. Phys.* **A 710** (2002) 180 [hep-ph/0205151].

[17] J. Raufeisen and J.-C. Peng, *Relating parton model and color dipole formulation of heavy quark hadroproduction*, *Phys. Rev.* **D 67** (2003) 054008 [hep-ph/0211422].

[18] I. Balitsky, *Operator expansion for high-energy scattering*, *Nucl. Phys.* **B 463** (1996) 99 [hep-ph/9509348];
J. Jalilian-Marian, A. Kovner, A. Leonidov and H. Weigert, *The Wilson renormalization group for low x physics: towards the high density regime*, *Phys. Rev.* **D 59** (1999) 014014 [hep-ph/9706377] [*ibid.* **59** (1999) 014015] [*ibid.* **59** (1999) 034007];
E. Iancu, A. Leonidov and L.D. McLerran, *Nonlinear gluon evolution in the color glass condensate. I*, *Nucl. Phys.* **A 692** (2001) 583 [hep-ph/0011241];
H. Weigert, *Unitarity at small Bjorken x*, *Nucl. Phys.* **A 703** (2002) 823 [hep-ph/0004044].

[19] Y.V. Kovchegov, *Small-x F_2 structure function of a nucleus including multiple Pomeron exchanges*, prd601999034008.

[20] E. Iancu, K. Itakura and S. Munier, *Saturation and BFKL dynamics in the HERA data at small x*, *Phys. Lett.* **B 590** (2004) 199 [hep-ph/0310338].

[21] N. Armesto, *A simple model for nuclear structure functions at small x in the dipole picture*, *Eur. Phys. J.* **C 26** (2002) 35 [hep-ph/0206017].

[22] A.I. Shoshi, F.D. Steffen and H.J. Pirner, *S-matrix unitarity, impact parameter profiles, gluon saturation and high-energy scattering*, *Nucl. Phys.* **A 709** (2002) 131 [hep-ph/0202012].

[23] A.M. Stasto, K. Golec-Biernat and J. Kwiecinski, *Geometric scaling for the total γp cross-section in the low x region*, *Phys. Rev. Lett.* **86** (2001) 596 [hep-ph/0007192].

[24] V.P. Goncalves and M.V.T. Machado, *Geometric scaling in inclusive charm production*, *Phys. Rev. Lett.* **91** (2003) 202002 [hep-ph/0307090].

[25] H1 collaboration, C. Adloff et al., *Measurement of open beauty production at HERA*, *Phys. Lett.* **B 467** (1999) 156 [hep-ex/9909029].

H1 collaboration, C. Adloff et al., *Measurement of open beauty production at HERA*, *Phys. Lett.* **B 467** (1999) 156 [hep-ex/9909029].

[26] M.S. Atiya et al., *Evidence for the high-energy photoproduction of charmed mesons*, *Phys. Rev. Lett.* **43** (1979) 414;
D. Aston et al., *Photoproduction of charmed D mesons at gamma energies of 40 GeV to 70 GeV*, *Phys. Lett.* **B 94** (1980) 113;
EUROPEAN MUON collaboration, J.J. Aubert et al., *Production of charmed particles in 250 GeV μ^+ - Iron interactions*, *Nucl. Phys.* **B 213** (1983) 31;
K. Abe et al., *Charm photoproduction cross-section at 20 GeV*, *Phys. Rev. Lett.* **51** (1983) 156;
SLAC HYBRID FACILITY PHOTON collaboration, K. Abe et al., *Lifetimes, cross-sections and production mechanisms of charmed particles produced by 20 GeV photons*, *Phys. Rev.* **D 33** (1986) 1;
PHOTON EMULSION collaboration, M.I. Adamovich et al., *Cross-sections and some features of charm photoproduction at gamma energies of 20 GeV to 70 GeV*, *Phys. Lett.* **B 187** (1987) 437;
TAGGED PHOTON SPECTROMETER collaboration, J.C. Anjos et al., *Photon-gluon fusion analysis of charm photoproduction*, *Phys. Rev. Lett.* **65** (1990) 2503;
EUROPEAN MUON collaboration, J.J. Aubert et al., *Observation of wrong sign trimuon events in 250 GeV muon-nucleon interactions*, *Phys. Lett.* **B 106** (1981) 419.

[27] S. Munier, *Geometric scaling in a symmetric saturation model*, *Phys. Rev.* **D 66** (2002) 114012 [hep-ph/0205319].

[28] N. Armesto, C.A. Salgado and U.A. Wiedemann, *Relating high-energy lepton hadron, proton nucleus and nucleus nucleus collisions through geometric scaling*, *Phys. Rev. Lett.* **94** (2005) 022002 [hep-ph/0407018].

[29] A.D. Martin, R.G. Roberts, W.J. Stirling and R.S. Thorne, *Physical gluons and high-e(t) jets*, *Phys. Lett.* **B 604** (2004) 61 [hep-ph/0410230].

[30] FERMILAB E653 collaboration, K. Kodama et al., *Charm meson production in 800 GeV/c proton-emulsion interactions*, *Phys. Lett.* **B 263** (1991) 573;
R. Ammar et al., *D-meson production in 800 GeV/c p pinteractions*, *Phys. Rev. Lett.* **61** (1988) 2185;
LEBC-EHS collaboration, M. Aguilar-Benitez et al., *Charm hadron properties in 400 GeV/c p p interactions*, *Z. Physik* **C 40** (1988) 321;
E769 collaboration, G.A. Alves et al., *Forward cross-sections for production of D^+, D_0, D/s, $D*+$ and λ/c in 250 GeV $\pi^\pm$, $k^\pm$ and p nucleon interactions*, *Phys. Rev. Lett.* **77** (1996) 2388 [Erratum *ibid.* **81** (1998) 1537];

ACCMOR collaboration, S. Barlag et al., *Production of $D, D*$ and $D(S)$ mesons in 200 GeV/c π^-, k^- and ψ interactions*, *Z. Physik* **C 39** (1988) 451;

PHENIX collaboration, K. Adcox et al., *Measurement of single electrons and implications for charm production in $Au + Au$ collisions at $S(N)^{(1/2)} = 130$ GeV*, *Phys. Rev. Lett.* **88** (2002) 192303 [nucl-ex/0202002];

O. Botner et al., *Production of prompt electrons in the charm p_T region at $\sqrt{s} = 630$ GeV*, *Phys. Lett.* **B 236** (1990) 488.

Erratum

In the original version of this paper, there are two misprints in table 1, which gives the parameters of the fit to the differential cross section $x_F \, d\sigma/dx_F$ for charm production in proton-air collisions. The corrected table 1 appears below. We also call attention that the parameterization is valid in the interval $10^4 < E_p \leq 10^{11}$ GeV and $0.05 \leq x_F \leq 0.8$.

Energy Range	a_0	a_1	b_0	b_1	n_0	n_1
$10^4 < E_p < 10^8$ GeV	6804 μb	822	0.05	0.016	7.5	-0.107
$10^8 < E_p < 10^{11}$ GeV	5422 μb	403	0.025	0.023	6.7	-0.102

Table 3: Parameters of the fit to the differential cross section $x_F \, d\sigma/dx_F$ for charm production in proton-air collisions (see text).

Added acknowledgments